Applied Science, Computing and Energy, 2026, 4(3), 01-18

Evaluation of Maximum Allowable Power Density and Thermal Limitations of Fuel Assembly of the Miniature Neutron Source Reactor as a Tool for Its Core Performance Measurements

Anas Muhammad Salisu, Joseph Istipanus Abaleni, Yusuf Aminu Ahmed, Nasiru Rabiu, and Jamilu Abdullahi Yusuf

Received: 12 December 2025/Accepted: 30 January 2026 /Published: 20 February 2026

Abstract: *The ratio of peak heat flux to the average heat flux around a reactor core is known to be the Power Peaking Factor of the reactor. This parameter was reported to be the key value that dictates the maximum allowable power density of a fuel assembly. Investigation shows that reactor core performance largely depends on the power peaking factor. It was in recognition of the role of this parameter that measurements were performed in this work to verify the Power Peaking Factor and core performance of the Nigeria Research Reactor–1 (NIRR-1) core, which is a Miniature Neutron Source Reactor (MNSR). Our results show that the Power Peaking Factor for a preset neutron flux of* 5.0×10^{11} $cm^{-2}s^{-1}$ *ranges from* 0.707 ± 0.293 *to* 1.014 ± 0.014 *with an average coolant temperature difference of 12.1˚C. This agrees with the inherent feature of MNSRs that compensates for the high negative temperature coefficient of reactivity in order to keep the reactor stable at its preset power level. This is also in agreement with the safety requirements of the MNSR, which does not permit power excursion and occurrence of boiling. However, our results show that the reactor stability is not applicable during startup and shutdown conditions. It means that utilization of the Reactor must wait some few minutes after startup to achieve stability and must stop some few minutes before the shutdown. The results also indicate the need to obtain a correction factor for samples that will stay in the reactor for a cyclic or longer period of irradiation provided there will be shut down and start-up in between the irradiations. Our results also revealed that there is a strong dependence of the reactor power on coolant temperature and rod position, which is in perfect agreement with the design of the MNSR and findings of many workers in the area. The computer program developed in this work for the determination of power peaking factor using moderator parameters will not only serve as a new source code for microcomputer control of the reactor peak power, maximum power factor and flux distribution but will also make it possible for the microcomputer console to display real time peak power level, maximum power factor thermal limitation of the reactor core, a tool that is lacking in MNSR design.*

Keywords*: Core Performance, Power Peaking Factor, Thermal Limitations, MNSR, NIRR-1*

Anas Muhammad Salisu*
Physics Department Ahmadu Bello University Zaria Kaduna State Nigeria
Email: abuumair399@gmail.comm
https://orcid.org/0000-0002-3186-4595

Joseph Istipanus Abaleni
Department of Physics, Kaduna State College of Education, Gidan Waya, Kaduna State, Nigeria
Email: abaleni30@gmail.com
https://orcid.org/0009-0004-3789-4332

Yusuf Aminu Ahmed
Centre for Energy Research and Training, Ahmadu Bello University, Zaria, Nigeria
Email: yaahmed1@gmail.com
https://orcid.org/0000-0001-6342-2401

Nasiru Rabiu
Physics Department, Ahmadu Bello University, Zaria, Nigeria
Email: nrabiu@yahoo.com
https://orcid.org/0000-0002-2491-6326

Jamilu Abdullahi Yusuf
Centre for Energy Research and Training, Ahmadu Bello University, Zaria-Nigeria
Email: yusufjameelx@gmail.com
https://orcid.org/0000-0002-1904-3241

1.0 Introduction

The power peaking factor, defined as the ratio of maximum local power density to the average core power density, is a critical safety parameter that governs thermal margins and fuel integrity in nuclear reactors (Sobes *et al*., 2011, Souza *et al*., 2006, Guosheng, 1993a and 1993b) Khamis *et al*. 2007). In a light water moderated reactor, the fuel assembly usually consists of only one type fuel element and enrichment, with the corner fuel rod nearest to the cruciform water gap generating the highest power density in the assembly. The ratio between the highest power and that averaged over the assembly is called the local power peaking factor (PF), and is a key value that dictates the maximum allowable power density of the assembly (Ranvik, 1990 and 1992). Investigation shows that reactor core performance largely depends on the power peaking factor of the core assembly (Sobes *et al*., 2011, Souza *et al*., 2006, Guosheng, 1993a and 1993b)).

Several attempts were made previously to depress the local power peaking factor by flattening the power distribution to depress the power peaking factor through the lowering of fuel enrichment at the corners of the core. The other alternative used is the impairment of the neutron multiplication factor with the use of too many fuel rods with low enrichment (Vladimir *et al*., 2011). These two approaches were shown to optimize the enrichment distribution within the fuel assemblies. Despite these contributions, these studies primarily focused on design optimization and burn-up behavior, without direct experimental evaluation of the power peaking factor or its coupling with thermal–hydraulic parameters

The Nigeria Research Reactor-1 (NIRR-1) is a low power, light water moderated, Miniature Neutron Source Reactor (MNSR) from China Institute of Atomic Energy, Beijing (Gao *et al*., 1992). Just like other MNSRs, NIRR-1 has a small core of 23cm^2 with 347 fuel elements arranged in 10 concentric circles. The reactor was built with a single control rod which performs both regulatory and shim functions. In case of rod stuck in fully out position, reactor shutdown will only be achieved by pumping cadmium or lowering into any of the inner irradiation channels near the core. This design created an opportunity for single point of failure as it does not allow for redundancy. In addition, the single rod design brought about concerns on safety of the MNSR in the event of rod drive mechanism fault or electrical system failure. However, these concerns were usually addressed through the in-built negative temperature coefficient of reactivity of the reactor, which does not permit power excursion. Detailed descriptions of the reactor parameters and its auxiliary facilities were reported in our earlier publications (Ahmed *et al*., 2008; 2011; 2013).

Since the commissioning of NIRR-1 in 2004, several experiments were conducted to measure its safety parameters. The flux stability test was done (Musa, *et al*., 2012), flux variation measurements were performed (Ahmed, *et al*., 2008), maximum operable time was determined (Ahmed *et al*., 2011) and effects of poisoning evaluated (Ahmed, *et al*., 2012). However, little effort was made to determine the reactor's power peaking factor. Other MNSR groups like Khamis & Alhalabi (2007), and Abrefah *et al*., 2010 have demonstrated the dependence of neutron flux and power of MNSR on thermal hydraulic parameters where they have reported that the flux values could be exploited to predict the reactor power and flux distribution. Some of the groups (Khattab, 2005; Haddad, 2009; Khan *et al*., 2009) did intensive work on burn-

up calculation and monitoring. However, they did not extend their works to power peaking factor and its relationship with the thermal hydraulic parameters.

Earlier on, the Chinese group (Jang *et al*. 2001) used trained neural networks to predict the power in each fuel channel for typical $1/8^{th}$ core symmetry of a PWR Reactor. They then applied simulated annealing to optimize the fuel loading of the PWRs. Using a different approach, Zhang *et al*. 1984 described an application of a linear superposition model (LSM) for estimating the power and physics parameters of such reactors.

Monte Carlo modeling of a PBMR-400 was done by Vladimir. et al. 2011 to determine individual pebble temperature peaking factor due to local pebble arrangement in a pebble bed reactor core. In their work they concluded that the stochastic nature of the pebble bed cannot lead to highly elevated fuel temperatures but rather local or core-wide coolant flow reductions are the likely cause. These findings attract a lot of attention on whether to determine individual or collective power peaking factors of reactor fuel elements. However, since NIRR-1 core is a sealed one with no online refueling, a collective determination of the power peaking factor is more desirable and yields more accurate values.

Another attempt is by Shima & Ali (2013) who studied axial variation of enrichment distribution method and radial variation of enrichment distribution in VVER/1000 reactor using a Hopfield neural network to optimize fuel management. They investigated appropriate ways to solve the problem of optimizing fuel management in VVER/1000 reactor. They suggested the use of coupled programs, which one of which is the nuclear code, for making a database and modeling the core, and another one is Hopfield Neural Network Artificial (HNNA), all in an effort to estimate the fuel power density.

Our group have earlier reported that the neutron flux distribution in the core of the MNSR determines the power and dynamic behavior of the reactor (Ahmed *et*. *al*., 2008). It has been shown that the thermal neutron flux achieves its maximum value in the center of the reactor core and falls to zero at the extreme ends of the core since very few thermal neutrons are produced at the extreme ends (Ravnik, 1990; Abrefah *et*. *al*., 2011; Musa *et*. *al*., 2013). It has also been shown that research reactor flux stability is a requirement for neutron activation analysis and precious stone irradiation (Desorte *et al*., 1972; Kapsimalis *et al*., 2009; Ahmed *et al*., 2010; 2013). However, the average flux of a reactor is a variable parameter that depends on the reactor's moderator and coolant temperature. These parameters need to be monitored from time to time to establish the stability of the reactor's flux.

In 2012, in an attempt to characterized the newly installed cadmium-lined irradiation channel in NIRR-1 MNSR, we determined the radial and axial neutron flux distribution in the irradiation channel of the reactor using foil activation technique (Musa *et al*. 2012). Our results show that the installed cadmium line did not affect NIRR-1 flux stability. We have also reported the process and procedures used in the lining of the irradiation channel with cadmium and the performance of the reactor afterwards (Ahmed, *et.al*., 2013).

In an effort to characterize the relationship of coolant and thermal power of the reactor, we used an experimental method to test the coolant flow rate and velocity in the core of the MNSR (Agbo, *et.al*., 2015A) and the heat balance method in the thermal power calibration (Agbo *et.al*., 2015B). During this period, the international community has undertaken analyses for supporting the MNSR conversion from use of High Enriched Uranium Core to Low Enriched Uranium core (IAEA-TECDOC-1844). The processes of the conversion of the Nigeria Research Reactor-1

MNSR will be reported in another publication but we have published the impact of the conversion on the reactor thermal power calibration (Asuku, *et.al*., 2020).

In addition, our group have gone further to estimate the burn-up and core life time expectancy of the MNSR using the WIMS and CITATION codes (Yahya, *et. al*., 2017), analysed the thermal power calibration methods for the MNSR (Agbo, *et. al*., 2017), determined the effect of coolant temperature on the reactor's power behaviour (Ahmed *et. al*., 2011; Anas *et.al*., 2017) and used positive period method in the calibration and determination of integral worth of the MNSR control rod (Asuku, *et.al*., 2015).

From the foregoing review, a clear gap exists in the experimental determination of the power peaking factor for NIRR-1 and its integration with thermal–hydraulic performance indicators such as coolant temperature rise and heat removal capability. Additionally, the absence of a simple, reactor-specific computational tool for real-time assessment of these parameters limits operational safety analysis. Following the successes of the above efforts, in this work, we ventured into the determination of the reactor's power peaking factor and thermal limitation on its core performance. The objectives are to use coolant temperature values and other reactor parameters to develop a simple thermal-hydraulic computer program and deploy the program to obtain both the maximum power factor and the thermal limitations of its core. It is our hope that the work will be a viable tool in the determination of the power peaking factor and core performance of a miniature neutron source reactor.

2.0 Theoretical Considerations

The power peaking factor represents the maximum power factor among all the fuel rod in the studied assembly. It is a relative power value which is calculated according to the equation. The thermal hydraulic design of the reactor core is done for the maximum power (not only for the average power), thus it is better to use new quantity "power peaking factor" which is defined as:

PPF = (maximum power density)/ (average power density)

$$PPF = \left(P_{fuel} - P_{av}\right)/P_{av} \quad (1)$$

In the equation above, P_{fuel} represent the power in the specific fuel; P_{av} represents the average power of the whole fuel assembly. So, the power peaking factor, PPF, can be either positive or negative, and it clearly shows the power magnitude of each fuel rod.

The fuel assembly consists of a group of fuel cells. It is considered that each fuel cell consists on a rectangular parallelepiped of height *H* and sides "*a*" and "*b*", as illustrated in Fig. 1. Also, the cells are homogenized; i.e., the material composition is in a homogeneous form (only for purposes of presenting the main ideas of the proposed method). The cells present a critical condition and the boundary condition is that the neutron flux is zero. In the case of these cells, the neutron flux is carried out through the solution of the Helmholtz equation below:

$$\nabla^2\phi(r) + B_g^2\phi(r) = 0. \quad (2)$$

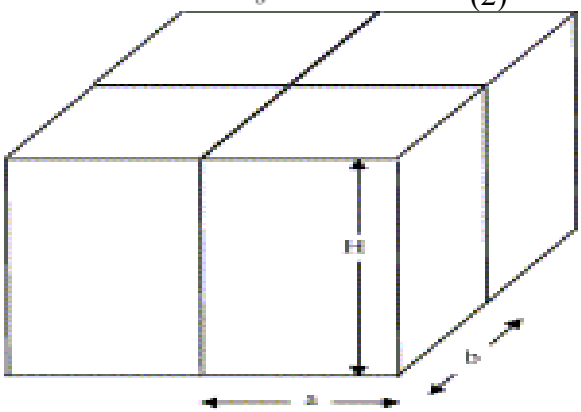

Fig. 1: Fuel assembly formed by a set of fuel cell.

The boundary conditions for the neutron flux are (Sobes *et al*., 2011, Souza *et al*., 2006, Guosheng, 1993a and 1993b):

$$\phi(a,y,z) = \phi(x,b,z) = \phi(x,y,H) = 0, \quad (1)$$

where B_g =:is the geometric buckling.

The solution of the Helmholtz equation for the neutron flux with the previous conditions for the cells is:

$$\phi(r) = \cos\left(\frac{\pi x}{a}\right)\cos\left(\frac{\pi y}{b}\right)\cos\left(\frac{\pi z}{H}\right), \quad (3)$$

And the solution for k_∞ is:

$$k_\infty = \frac{\nu N_f \sigma_f}{N_a \sigma_a}\frac{1}{1+L^2 B_g^2}, \quad (4)$$

where ν =: is the average number of neutrons released per fission, N_f =: is the number density of fissile nuclei or fissile content, σ_f =: is the microscopic fission cross section, N_a =: is the number density of absorption nuclei, σ_a =: is the microscopic absorption cross section, L =: is the diffusion length. For the rectangular parallelepiped cell, and B_g =: is the geometric buckling.

$$B_g^2 = \left(\frac{\pi}{a}\right)^2 + \left(\frac{\pi}{b}\right)^2 + \left(\frac{\pi}{H}\right)^2. \quad (4)$$

The term $1/(1+L^2B_g^2)$ in Eq. (4) is the no-leakage probability of the neutrons (P_{NL}). This term presents values close to 1.0. Therefore, with an approximation, k_∞ is:

$$k_\infty = \frac{\nu N_f \sigma_f}{N_a \sigma_a}. \quad (5)$$

It should be noted that this reactor flux distribution in a radial direction normally peaks in the center and the radial power peaking factor is typically 1.65.

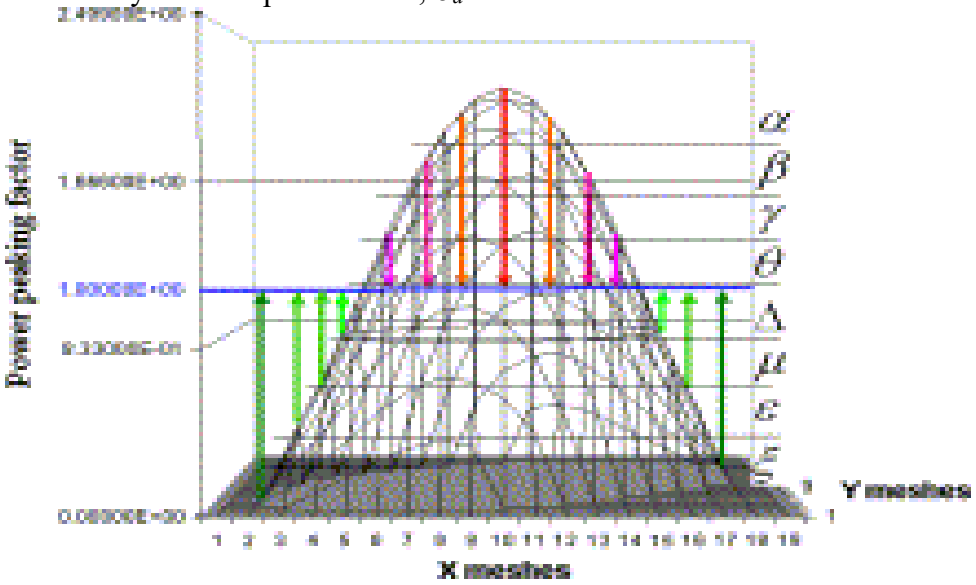

Fig. 2: The reactor core zoning based on the distribution of the core's radial power peaking factor with the averaged enrichment (Guosheng, 1993a and 1993b)

The weighting factor for each type of the fuel assembly based on their fuel compositions, where the coupling codes were used to calculate the thermal power produced by each fuel assembly is thus (Sobes *et al*., 2011, Souza *et al*., 2006, Guosheng, 1993a and 1993b):

$$C_i = \frac{P_i}{P_{ave}} \quad (6)$$

where C_i =: is the weighting factor value, i represents the type of fuel assemblies; P_i =: is the produced thermal power in each type of fuel assembly; and P_{ave}=: is

the produced power of the fuel assembly with the averaged enrichment.

In order to calculate the weighting factor, we assumed an equal neutron flux in the numerator and denominator of this formula; as a result, the neutron flux parameter was removed from both the numerator and denominator of this correlation. Then, to calculate the geometrical weighting factor (the "G" factor) of the m positions of the core, the whole reactor core was loaded based on the averaged fuel composition, and the radial power peaking factor was obtained from positions accordingly (Guosheng, 1993a and 1993b):

$$G_m = 163\frac{P_m}{\sum_{m=1}^{163} P_m} \quad (7)$$

where m = the number of fuel assemblies, m=163 and P_m is the produced thermal power of each fuel assembly.

The equation that depictsthe relation amongst core inlet temperature, temperature difference and power level as obtained from a simulation experiment on MNSR is expressed in the form (Shi, 1990)

$$\Delta T = (5.725 + 147.6H^{-2.64})T_i^{-0.35}P^{(0.59+0.0091T_i)} \quad (8)$$

where ΔT = temperature difference between the inlet and outlet orifice (℃), H = Height of the inlet orifice (mm), and T_i = inlet temperature (℃)

The design of the inlet orifice of MNSR was made to be 6mm for safety and technical reasons (Yang, 1990; Ahmed *et al*., 2008). Therefore subtituting the value of H into equation (8) reduces the equation to:

$$\Delta T = 7.04T_i^{-0.35}P^{(0.59+0.0091T_i)} \quad (9)$$

Thus $$P = Exp\left[Ln\left(\frac{\Delta T}{7.04T_i^{-0.35}}\right)((0.59 + 0.0091T_i))^{-1}\right] \quad (10)$$

For a fixed height of inlet orifice, it is expected from equation 10 that the reactor power varies linearly with temperature. The power peaking factor for each type of the fuel assembly based on their fuel compositions, where the coupling codes were used to calculate the thermal power produced by each fuel assembly (equation 10). The maximum power factor produced in reactor core is given by equation 6. We thus applied equation (6) and (10) The aim of this study is to determine the power peaking factor of NIRR-1 and evaluate its thermal–hydraulic implications through experimental analysis and computational modeling. Specifically, the study develops a simplified thermal–hydraulic computer program applicable to MNSR-type reactors.

The findings of this study enhance reactor safety evaluation, provide a practical tool for reactor operators, and contribute to improved real-time monitoring of thermal limits in miniature neutron source reactors.

3.0 Experimental Methodology

The Nigerian Research Reactor–1 was operated at different days at a preset flux value of 5×10^{11} n cm^{-2} s^{-1} and the control rod position was limited to 220 mm. This makes the reactor operate at half of its expected installed capacity. Readings were taken after every twenty minutes for six hours and were tabulated in Tables 2 to 7. The mass of the irradiated fuel assembly of the NIRR-1 MNSR used in this study, including the Plutonium weight and mass of fission products, is shown in Table 1 and the core of the MNSR is shown in Fig. 2

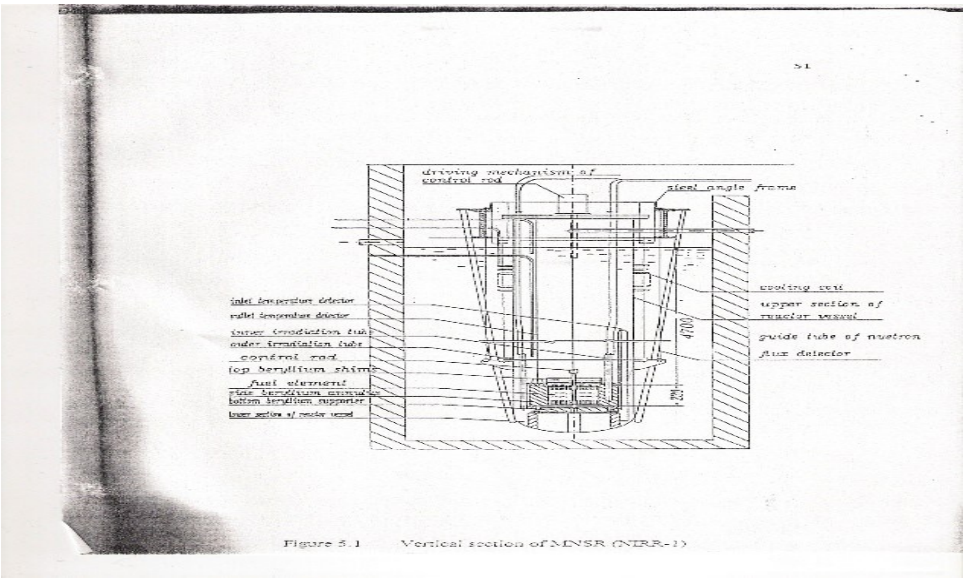

Fig. 2: Vertical Section of MNSR Core

Table 1: Irradiated HEU Fuel Assembly of NIRR-1 MNSR

Item	Mass of Fresh Fuel (g)	Total Pu weight (g)	Mass of Fission Product (g)	Total weight (g)
HEU Core + Al Matrix	5964.610	0.129	15.730	5980.469
Fresh Fuel Pin #1	17.189	NA	NA	17.189
Fresh Fuel Pin #2	17.189	NA	NA	17.189
Fresh Fuel Pin #3	17.189	NA	NA	17.189
Mass of Grid Plates	NA	NA	NA	327.900
Mass of Guide Tube	NA	NA	NA	54.200
Mass of end Plugs	NA	NA	NA	397.200
			Total	**6811.336**

Mass of Fresh Fuel = Mass of Fresh U + Al Matrix (1104.610 + 4860) g = 5964.610g
But mass of fresh fuel per pin = 1104.61 + 4860/347 = 17.189g

A simple computer program was then developed using Netbeans IDE 7.4 (a Java application) software based on the temperature difference equation of power (equation 10) to determine peak power, maximum power factor and flux distribution. It also made it possible for the microcomputer console to display real-time peak power level, maximum power factor and thermal limitation of the reactor core, a tool that is lacking in MNSR design. Details of the program can be obtained from NIRR-1 laboratory at the Centre for Energy Research and Training, Ahmadu Bello University, Zaria, Nigeria.

When the reactor is operating at a neutron flux value of 5×10^{11} n cm^2s^{-1}, the inlet and outlet temperatures of the coolant were

recorded after every twenty minutes for about six hours, and the temperature difference between the two was evaluated. This enabled the investigation of the following:

a) If there is a fairly constant reactor power and flux distribution with a temperature difference.
b) If the temperature difference recorded during the operation is fairly constant with time.
c) If there is a steady rise in the inlet and outlet temperature with time.
d) If there is insufficient thermal circulation of coolant in the core.

4.0 Results and Discussions

The results obtained in this work are hereby presented in Tables 2 to 7. All measurements were done at a preset flux value of 5×10^{11} n cm^2 $s^{-1,}$ representing reactor power of 15KW in order to study the contributions of the temperature coefficient of reactivity on the reactor power stability. Just before the commencement of the experimental work and the process of reactor start up, it was observed that the inlet and the outlet temperatures were all at room temperatures (24.2˚C and 24.5 ˚C respectively). These values indicate complete cooling of the reactor during the long shutdown period that preceded this work. At start-up, the corresponding power peaking factor was 0.0027, indicating minimal deviation between local and average power, consistent with earlier predictions by In Ho Bae *et al*. (2009) and Vladimir *et al*. (2011). However, a few minutes after the startup of the reactor, the outlet temperature picks up rapidly to an average of 37.1 ˚C, yielding a temperature difference of 13.0 ˚C. These temperature values gave rise to a sharp increase in power peaking factor due to the inherent features of the reactor, and according to the rule governing insertion of excess reactivity into the reactor by the withdrawal of the control rod during the startup.

The data presented in Table 3 were collected over six hours on a different day from those in Table 2. The inlet and outlet temperatures exceeded 25.0 °C and 37.6 °C, respectively, reflecting incomplete cooling of the reactor core due to the relatively short shutdown period preceding the measurements This is in recognition of the fact that the reactor was operated not quite long (to obtain the readings in Table 1) and the coolant not completely cooled during the few days of the shutdown. These values gave an average outlet temperature of 37.6 ˚C and a temperature difference of 12.6˚C. These temperature values gave rise to a sharp increase in power peaking factor due to the inherent features of the reactor and according to the rules governing insertion of excess reactivity into the reactor by the withdrawal of the control rod during the startup. As the inlet and outlet temperature values increase with an increase in control rod withdrawal the Power Peaking Factor oscillates around 1.00 indicating that there was no rise in the different between average power and preset values.

During reactor shutdown, although inlet and outlet temperatures remained relatively stable, the power peaking factor decreased sharply from 1.03 to 0.19, reflecting the withdrawal of excess reactivity through control rod insertion while the preset flux remained constant. This is an indication that there is no difference between average power and preset power values. This trend continued until the reactor was shut down. Even though the inlet and outlet temperature remain steady while the reactor is being shut down, the power peaking factor drastically reduces from 1.03 to 0.19, responding to the withdrawal of excess reactivity by the control rod insertion during the shutdown stage. This is also in agreement with the fact that the

average power is gradually being reduced by the control rod while the preset flux remains constant.

Table 2: Values of reactor power peaking factor obtained using measured inlet temperatures and the values of coolant temperature rise at a neutron flux of 5×10^{11} $cm^{-2}s^{-1}$

Time (Hrs)	Inlet Tempt (˚C)	Outlet Tempt (˚C)	Coolant Tempt (˚C)	Predicted Power (KW)	Power Peaking Factor	Standard Deviation	Percentage Error %
1.5	24.2	24.5	0.30	0.0404	0.0027	0.9973	99.73
1.6	24.1	37.1	13.0	15.1271	1.0085	-0.0085	0.85
1.8	26.0	38.9	12.9	15.3423	1.0228	-0.0228	2.28
2.0	27.0	40.1	13.1	15.9126	1.0608	-0.0608	6.08
2.2	28.4	40.6	12.2	14.4779	0.9652	0.0348	3.48
2.4	28.9	40.6	12.6	15.3051	1.0203	-0.0203	2.03
2.4	28.6	41.3	12.7	15.4437	1.0296	-0.0296	2.96
2.4	29.1	33.3	4.20	2.7949	0.1863	0.8137	81.37
Average	27	37	10.1	10.6075	0.7072	0.2928	29.28

Table 3: Values of reactor power peaking factor obtained using measured inlet temperatures and the values of coolant temperature rise at a neutron flux of 5×10^{11} $cm^{-2}s^{-1}$

Time (Hrs)	Inlet Tempt. (˚C)	Outlet Tempt. (˚C)	Coolant Tempt. (˚C)	Predicted Power (KW)	Power Peaking Factor	Standard Deviation	Percentage Error %
09:50	26.3	38.4	12.1	13.9352	0.9290	0.0710	7.10
10:10	27.9	40.4	12.5	14.9496	0.9966	0.0034	0.34
10:30	29.3	41.7	12.4	14.9939	0.9996	0.0004	0.04
10:50	30.1	42.3	12.2	14.7424	0.9828	0.0172	1.72
11:10	30.2	42.7	12.5	15.3215	1.0214	-0.0214	2.14
11:30	31.6	44.0	12.4	15.3349	1.0223	-0.0223	2.23
11:50	31.9	43.9	12.0	14.6205	0.9747	0.0253	2.53
12:10	32.1	44.2	12.1	14.8346	0.9890	0.0110	1.10
12:30	32.2	44.1	11.9	14.4726	0.9648	0.0352	3.52
12:50	31.5	44.3	12.8	16.0880	1.0725	-0.0725	7.25
13:10	32.6	44.4	11.8	14.3367	0.9558	0.0442	4.42
13:30	32.7	45.2	12.5	15.6749	1.0450	-0.0450	4.50
13:50	32.2	44.1	11.9	14.4726	0.9648	0.0352	3.52
14:10	32.6	44.7	12.1	14.8996	0.9933	0.0067	0.67
14:30	32.6	44.9	12.3	15.2790	1.0186	-0.0186	1.86
14:50	33.0	44.9	11.9	14.5733	0.9716	0.0284	2.84
15:10	33.3	45.0	11.7	14.2357	0.9490	0.0510	5.10

15:30	33.1	45.2	12.1	14.9627	0.9975	0.0025	0.25
15:50	33.3	45.1	11.8	14.4224	0.9615	0.0385	3.85
Average	31.5	43.7	12.2	14.9423	0.9962	0.0038	0.38

Table 4: Values of reactor power peaking factor obtained using measured inlet temperatures and the values of coolant temperature rise at a neutron flux of 5 ×10^{11} cm^{-2} s^{-1}

Time (Hrs)	Inlet Tempt. (˚C)	Outlet Tempt. (˚C)	Coolant Tempt. (˚C)	Predicted Power (KW)	Power Peaking Factor	Standard Deviation	Percentage Error %
10:15	25.0	37.6	11.6	12.8147	0.8543	0.1457	14.57
10:40	27.6	39.9	12.3	14.5282	0.9685	0.0315	3.15
11:00	28.8	40.9	12.1	14.3579	0.9572	0.0428	4.28
11:20	29.8	41.8	12.0	14.3265	0.9551	0.0449	4.49
11:40	31.1	42.6	12.5	15.4545	1.0303	-0.0303	3.03
12:00	30.0	42.9	12.9	16.0538	1.0703	-0.0703	7.03
12:20	31.4	43.3	11.9	14.3673	0.9578	0.0422	4.22
12:40	31.4	43.4	12.0	14.5535	0.9702	0.0298	2.98
13:00	31.3	43.9	12.6	15.6743	1.0450	-0.0450	4.50
13:20	31.1	43.6	12.1	14.6992	0.9799	0.0201	2.01
13:40	31.3	43.6	12.1	14.7269	0.9818	0.0182	1.82
14:00	32.4	43.4	12.2	15.0629	1.0042	-0.0042	0.42
14:20	33.7	44.6	11.7	14.2829	0.9522	0.0478	4.78
14:40	32.2	44.4	12.3	15.2263	1.0151	-0.0151	1.51
15:00	32.5	44.5	11.7	14.1384	0.9426	0.0574	5.74
15:20	32.6	44.4	11.6	13.9657	0.9310	0.0690	6.90
15:40	33.0	44.8	11.8	14.3861	0.9591	0.0409	4.09
16:00	32.8	45.5	12.2	15.1145	1.0076	-0.0076	0.76
16:20	32.8	44.7	11.9	14.5360	0.9691	0.0309	3.09
Average	32.7	43.1	12.1	14.9123	0.9942	0.0058	0.58

Table 5: Values of reactor power peaking factor obtained using measured inlet temperatures and the values of coolant temperature rise at a neutron flux of 5×10^{11} cm^{-2} s^{-1}

Time (Hrs)	Inlet Tempt. (˚C)	Outlet Tempt. (˚C)	Coolant Tempt. (˚C)	Predicted Power (KW)	Power Peaking Factor	Standard Deviation	Percentage Error %
11:00	28.3	40.5	12.2	14.4616	0.9641	0.0386	3.86
11:20	30.2	42.3	12.1	14.5707	0.9714	0.0286	2.86
11:40	30.9	43.3	12.4	15.2357	1.0157	-0.0157	1.57
12:00	32.5	44.7	12.2	15.0759	1.0051	-0.0051	0.51
12:20	33.4	44.8	11.4	13.6924	0.9128	0.0872	8.72

12:40	33.1	45.3	12.2	15.1525	1.0102	-0.0102	1.02
13:00	33.7	46.0	12.3	15.4178	1.0279	-0.0279	2.79
13:20	33.9	45.8	11.9	14.6814	0.9788	0.0212	2.12
13:40	34.3	46.4	12.1	15.1072	1.0071	-0.0071	0.71
14:00	34.2	46.0	11.8	14.5278	0.9685	0.0315	3.15
14:20	34.5	46.9	11.4	13.8156	0.9210	0.0790	7.90
14:40	34.4	47.1	12.7	16.2775	1.0852	-0.0852	8.52
15:00	35.1	46.8	11.7	14.4397	0.9626	0.0374	3.47
15:20	33.5	47.0	12.5	15.7778	1.0519	0.0519	5.19
15:40	34.7	46.7	12.0	14.9627	0.9975	0.0025	0.25
16:00	35.9	47.5	12.6	16.2848	1.0837	-0.0837	8.37
16:20	35.3	47.6	12.3	15.6048	1.0403	-0.0403	4.03
16:40	35.4	47.8	12.4	15.8095	1.0540	-0.0540	5.38
17:00	35.3	47.7	12.4	15.7983	1.0532	-0.0532	5.32
Average	**33.6**	**45.8**	**12.2**	**15.2144**	**1.0143**	**-0.0140**	**1.43**

Table 6: Values of reactor power peaking factor obtained using measured inlet temperatures and the values of coolant temperature rise at a neutron flux of 5×10^{11} cm^{-2} s^{-1}

Time (Hrs)	Inlet Tempt. (˚C)	Outlet Tempt. (˚C)	Coolant Tempt. (˚C)	Predicted Power (KW)	Power Peaking Factor	Standard Deviation	Percentage Error %
11:50	28.7	40.8	12.1	14.3421	0.9561	0.0439	4.39
12:10	28.6	41.5	12.9	15.8227	1.0548	-0.0548	5.48
12:30	30.0	42.2	12.2	14.7275	0.9818	0.0182	1.82
12:50	30.7	42.8	12.1	14.6429	0.9761	0.0239	2.39
13:10	31.4	42.9	11.5	13.6307	0.9082	0.0918	9.18
13:30	32.0	44.3	12.3	15.1995	1.0133	-0.0133	1.33
13:50	31.8	44.5	12.7	15.9376	1.0625	-0.0625	6.25
14:10	31.2	44.6	13.4	17.2172	1.1478	-0.1478	14.78
14:30	32.1	44.4	12.3	15.2130	1.0142	-0.0142	1.42
14:50	32.5	45.0	13.5	17.6098	1.1740	-0.1740	17.4
15:10	33.5	44.9	11.4	13.7039	0.9136	0.0864	8.64
15:30	33.2	45.3	12.1	14.9751	0.9983	0.0017	0.17
15:50	33.0	45.0	12.0	14.7613	0.9841	0.0159	1.59
16:10	33.0	45.4	12.4	15.5219	1.0348	-0.0348	3.48
16:30	34.0	45.3	11.3	13.5767	0.9651	0.0349	3.49
16:50	34.1	44.1	10.0	11.2740	0.7516	0.2484	24.84
17:10	33.7	45.8	12.1	15.0362	1.0024	0.0024	0.24
17:30	34.8	46.4	11.6	14.2199	0.9480	0.0520	5.20
17:50	34.1	46.5	12.4	15.6586	1.0439	-0.0439	4.39

Average	32.2	44.3	12.1	14.8478	0.9899	0.0101	1.01

Table 7: Values of reactor power peaking factor obtained using measured inlet temperatures and the values of coolant temperature rise at a neutron flux of 5×10^{11} cm^{-2} s^{-1}

Time (Hrs)	Inlet Tempt. (˚C)	Outlet Tempt. (˚C)	Coolant Tempt. (˚C)	Predicted Power (KW)	Power Peaking Factor	Standard Deviation	Percentage Error %
10:50	27.3	40.6	13.3	16.3509	1.0901	-0.0901	9.01
11:00	29.0	40.9	11.9	14.0223	0.9348	0.0652	6.52
11:10	29.9	42.8	12.9	16.0379	1.0692	-0.0692	6.92
11:20	30.8	41.8	11.0	12.6538	0.8436	0.1564	15.64
11:30	30.5	43.2	12.7	15.7477	1.0498	-0.0498	4.98
11:40	31.9	43.4	11.5	13.6947	0.9130	0.0870	8.70
11:50	31.5	43.9	12.4	15.3209	1.0214	-0.0214	2.14
12:00	31.8	44.3	12.5	15.5534	1.0369	-0.0369	3.69
12:10	32.9	44.8	11.9	14.5609	0.9707	0.0293	2.93
12:20	33.5	45.5	12.0	14.8226	0.9882	0.0118	1.18
12:30	32.8	45.4	12.6	14.8808	1.0587	-0.0587	5.87
12:40	33.4	45.1	11.7	14.2476	0.9498	0.0502	5.02
12:50	33.7	45.1	11.4	13.7267	0.9151	0.0849	8.49
Average	31.5	43.7	12.2	14.9423	0.9962	0.0038	0.38

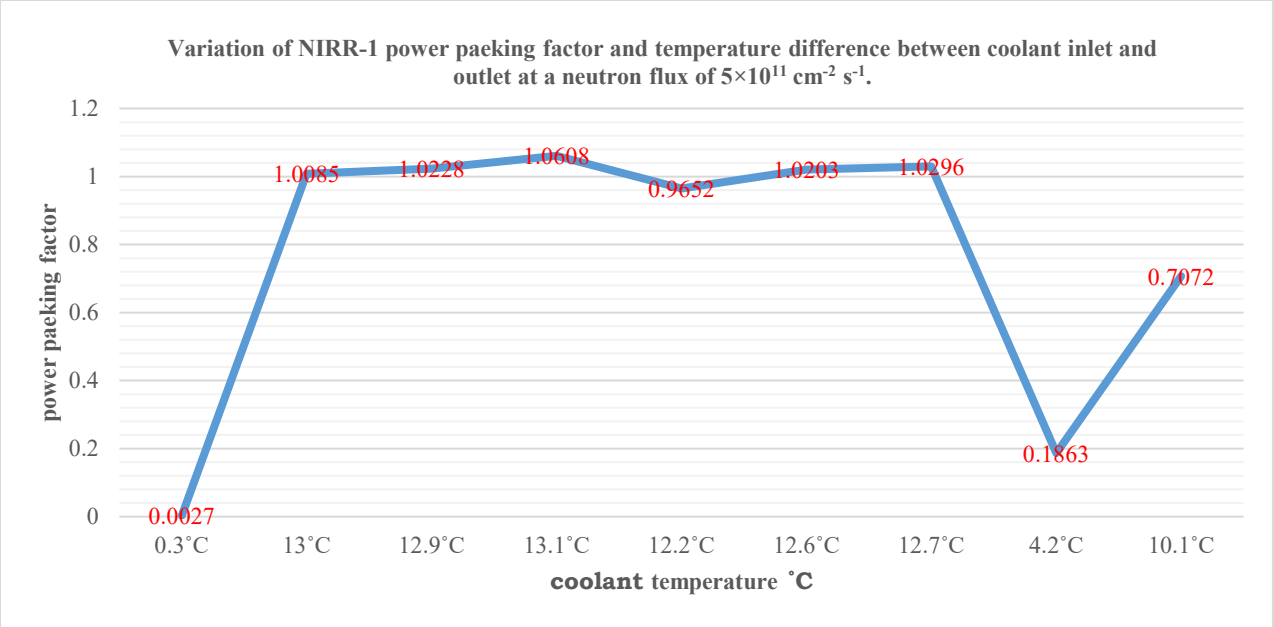

Fig.1: Variation of NIRR-1 power peaking factor and temperature difference between coolant inlet and outlet at a neutron flux of 5×10^{11} cm^{-2} s^{-1}

Fig. 1 illustrates the lower limits of the power peaking factor at the beginning and end of reactor operation. These deviations influence the average power peaking factor, which ideally approaches unity during steady-state operation. The figure also shows the oscillation of the Power Peaking Factor around 1.00 until shutdown.

Fig. 2 shows that the lower limits observed in Fig. 1 differ due to incomplete cooling during the brief non-operational period. However, this variation has no significant effect on the average power peaking factor, which continues to oscillate around unity up to shutdown

Although MNSR facilities are generally reported to exhibit high operational stability, the present results indicate that stability conditions are not fully established during reactor start-up and shutdown phases. Consequently, reactor utilization should commence only after a brief stabilization period following start-up and should cease before shutdown. The MNSR was reported by the manufacturers and some users to be stable. However, our results show that the Reactor's stability is not applicable during startup and shutdown conditions. It also shows that utilization of the Reactor must wait some few minutes after startup to achieve stability and must stop some few minutes before shutdown. These findings highlight the need for correction factors when irradiating samples under cyclic activation or prolonged irradiation conditions involving intermittent reactor shutdowns and restarts

Table 2 further demonstrates that extended reactor shutdown periods adversely affect start-up stability. It is therefore recommended that periodic test runs, preferably on a weekly basis, be conducted even in the absence of irradiation samples to maintain stable operating conditions.

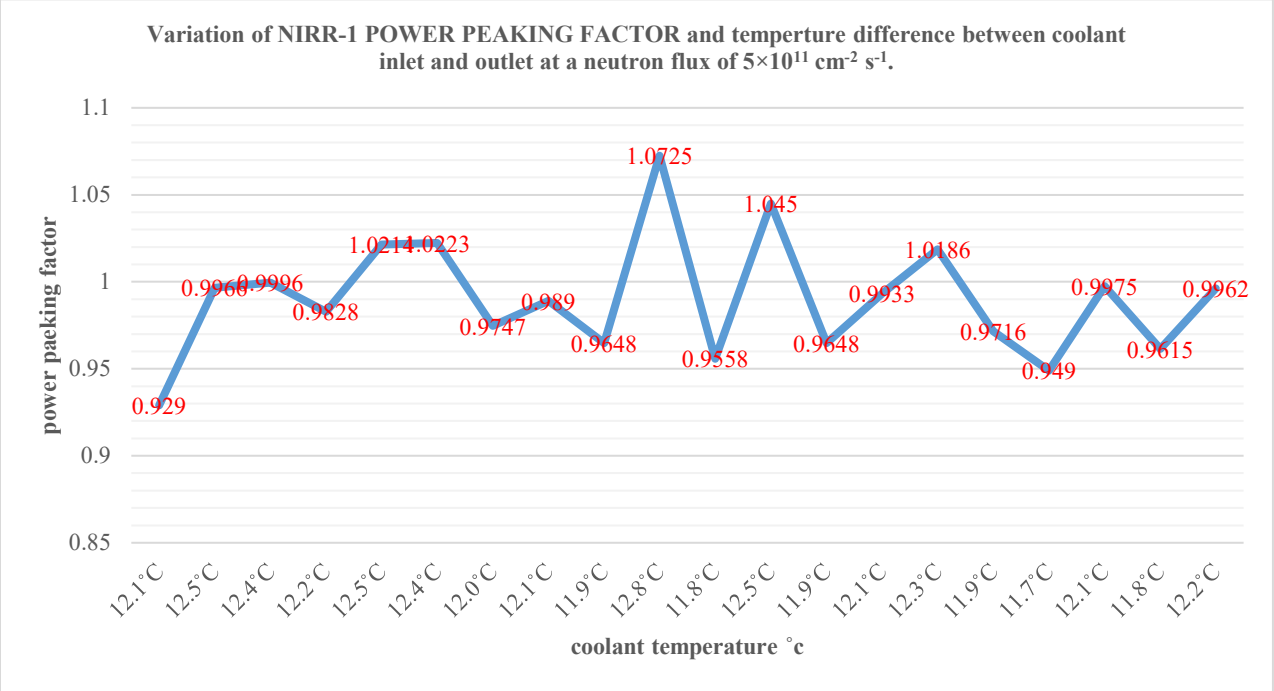

Fig. 2 Variation of NIRR-1 POWER PEAKING FACTOR and temperture difference between coolant inlet and outlet at a neutron flux of 5×10¹¹ cm⁻² s⁻¹

The results confirm that the reactor operated at a nearly constant power level of 15 kW throughout the experiment, with a steady temperature difference of approximately 12.1 °C. As shown in Tables 2–6, inlet and outlet temperatures increased gradually with time, yielding average values of 31.4 °C and 42.9 °C, respectively. This is due to the compact nature of the core, which was designed to cause restricted coolant circulation resulting from the compact core configuration in the core. These conditions represent optimal core performance for MNSR installations in tropical regions. Variations in ambient temperature may slightly influence inlet and outlet temperatures, thereby affecting allowable power density and fuel thermal limits. The inlet and outlet temperatures may, however, vary a little for regions with extreme temperature conditions, and that will affect the maximum allowable power density and thermal limitations of the fuel assembly. The results further indicate that the MNSR can be operated at half power (neutron flux of 5 × 10^{11} n cm^{-2} s^{-1}) in automatic mode for approximately eight continuous hours before fission product poisoning leads to maximum control rod insertion (232 mm), triggering automatic reactor shutdown. This observation agrees with the findings of Ahmed et al. (2011) and reflects the inherent safety features of the MNSR, including limited excess reactivity (<0.5 $, ≈4 mk) and a strong negative temperature coefficient of reactivity. This is in agreement with the findings of Ahmed *et al.* 2011. This, in combination with the limited MNSR excess reactivity that is less than 0.5$ (4mk) is another safety feature guaranteed by its in-build negative temperature coefficient of reactivity (Ahmed, *et al.* 2011), just in case the reactor is left unattended to for so long.

5.0 Conclusions

In this work, measurements were performed to determine the power peaking factor in the

Nigeria Research Reactor–1 core (NIRR-1), which is miniature neutron source reactor (MNSR) for the determination of its maximum allowable power density and thermal limitations of fuel assembly as a tool for core performance measurements. Our results show that the Power Peaking Factor for a preset neutron flux of 5.0×10^{11} $cm^{-2}s^{-1}$ ranges from 0.7072±0.2928 to 1.0143±0.0140. The average values of temperature difference recorded for all the experiments conducted were found to be constant with time and approximately equal to 12.1˚C for the whole period of operation. This indicates the optimum core performance of the reactor located at the tropical regions of the world. The temperature difference may vary a little for regions with extreme temperatures and that will affect the maximum allowable power density and thermal limitations of fuel assembly. This is an in-build feature of NIRR-1 that compensates for high negative temperature coefficient of reactivity in order to keep the reactor at its preset power level. The average Power Peaking Factor obtained is approximately 0.9982±0.0018. This shows that, the flux in the core of NIRR-1 is stable. This is in agreement with safety requirement of the reactor which does not permit power excursion and occurrence of boiling. The outcome of the above investigation is important in avoidance of power excursion and radiation exposure to personnel and the environment. The computer program developed in this work will serve as a new source code for microcomputer control of the reactor peak power, maximum power factor and flux distribution. It will also make it possible for the microcomputer console to display real time peak power level, maximum power factor thermal limitation of the reactor core, a tool that is lacking in MNSR design.

6.0 Acknowledgement

The Authors wish to acknowladge the cooperation and assistance of the NIRR-1 operation and utilization group during the experimental work. Special thanks to NIRR-1 Reactor Manager and the Director of the Centre for Energy Research and Training for permission to use NIRR-1 facilities.

7.0 References

Abrefah, R. G., Nyarko, B. J. B., Akaho, E. H. K., Sampong, S. A., & Sogbadji, R. B. M. (2010). Axial and radial distribution of thermal and epithermal neutron fluxes in irradiation channels of the Ghana Research Reactor-1 using foil activation analysis. *Annals of Nuclear Energy, 37*(8), 1027–1035.

Agbo, S. A., Ahmed, Y. A., Ewa, I. O. B., & Jibrin, Y. (2016). Analysis of Nigeria Research Reactor-1 (NIRR-1) thermal power calibration methods. *Nuclear Engineering and Technology, 48*(3), 673–683.

Agbo, S. A., Ahmed, Y. A., Ewa, I. O. B., Abubakar, M., & Anas, M. S. (2015). An experimental testing of coolant flow rate and velocity in the core of Nigeria Research Reactor-1. *International Journal of Nuclear Energy Science and Technology, 9*(2), 171–185.

Agbo, S. A., Ahmed, Y. A., Yahaya, B., & Iliyasu, U. (2015). The use of heat balance method in the thermal power calibration of Nigeria Research Reactor-1 (NIRR-1). *Progress in Nuclear Energy, 85*, 344–351.

Ahmed, Y. A., Balogun, G. I., Jonah, S. A., & Funtua, I. I. (2008). The behavior of reactor power and flux resulting from changes in core-coolant temperature for a miniature neutron source reactor. *Annals of Nuclear Energy, 35*(12), 2417–2419.

Ahmed, Y. A., Ewa, I. O. B., & Umar, I. M. (2002). Effective resonance energy and non-ideality of epithermal neutron flux distribution in neutron activation analysis. *Nigerian Journal of Physics, 14*(1), 82–85.

Ahmed, Y. A., Ewa, I. O. B., & Umar, I. M. (2006). Variations in nuclear data and its

impact on INAA. *Journal of Applied Sciences, 6*(8), 1692–1697.

Ahmed, Y. A., Landsberger, S., O'Kelly, D. J., Braisted, J., Gabdo, H., Ewa, I. O. B., Funtua, I. I., & Umar, I. M. (2010). Compton suppression method and epithermal NAA in the determination of nutrients and heavy metals in Nigerian food and beverages. *Applied Radiation and Isotopes, 68*(10), 1909–1914.

Ahmed, Y. A., Mansir, I. B., Yusuf, I., Balogun, G. I., & Jonah, S. A. (2011). Effects of core excess reactivity and coolant average temperature on maximum operable time of NIRR-1 miniature neutron source reactor. *Nuclear Engineering and Design, 241*(5), 1559–1564.

Ahmed, Y. A., Mansir, I. B., & Dewu, B. B. M. (2013). Installation of permanent cadmium-lined channel as a means for increasing epithermal NAA capabilities of miniature neutron source reactors. *Nuclear Engineering and Design, 263*, 70–76.

Anas, M. S., Ahmed, Y. A., Yusuf, S., & Yusuf, J. A. (2016). Effect of coolant temperature on core power behavior of a miniature neutron source reactor. *Journal of Nuclear Energy Science and Power Technology, 5*(3), 1–6.

Asuku, A., Ahmed, Y. A., Umar, A., Umar, S., Abdulmalik, N. F., & Abubakar, A. R. (2020). Impact of Nigeria Research Reactor-1 conversion on its thermal power calibration. *FUW Trends in Science & Technology Journal, 5*(2), 566–571.

Balogun, G. I., Jonah, S. A., Ahmed, Y. A., & Sa'adu, N. (2004). Results of on-site zero power and criticality experiments for the Nigeria Research Reactor-1 (Internal Report CERT/NIRR-1/ZP/01).

Ellis, R. J., Gehin, J. C., & Primm, R. T. (2006). Cross section generation and physics modeling in a feasibility study of the conversion of the high flux isotope reactor core to low enriched uranium fuel. American Nuclear Society.

Gao, Y., Gao, J., Tao, H., & Yang, Y. (1992). *Miniature neutron source reactor general description (MNSR Training Material MNSR-DC-1).* China Institute of Atomic Energy.

Guosheng, Z. (1993a). *Measurement for spatial neutron flux distribution (MNSR Training Material).* China Institute of Atomic Energy.

Guosheng, Z. (1993b). *Absolute neutron flux measurement by gold foil activation method (MNSR Training Material).* China Institute of Atomic Energy.

Haddad, K. H. (2009). Passive nondestructive burn-up monitoring of the MNSR irradiated fuel by measuring photo neutrons produced within fission products. *Applied Radiation and Isotopes, 67*(10), 1925–1929.

Han, S., Kim, U. S., & Seong, P. H. (1999). A methodology for benefit assessment of using in-core neutron detector signals in core protection calculator system (CPCS) for Korea standard nuclear power plants (KSNPP). *Annals of Nuclear Energy, 26*(6), 471–488.

In Ho Bae, Na, M. G., Yoon, J., & Park, G. C. (2009). Estimation of the power peaking factor in nuclear reactor using support vector machine and uncertainty analysis. *Nuclear Engineering and Technology, 41*(9).

International Atomic Energy Agency. (1990). *Practical aspects of operating a neutron activation analysis laboratory (IAEA-TECDOC-564).* IAEA.

International Atomic Energy Agency. (2018). *Analyses supporting conversion of research reactors from high enriched uranium fuel to low enriched uranium fuel: The case of miniature neutron source reactors (IAEA-TECDOC-1844).* IAEA.

Kapsimalis, R., Landsberger, S., & Ahmed, Y. A. (2009). The determination of uranium in food samples by Compton suppression epithermal neutron activation analysis. *Applied Radiation and Isotopes, 67*(11), 2097–2099.

Khamis, I. (2007). Assessment of cooling effect on extending the maximum operating time for the Syrian Miniature Neutron Source Reactor. *Progress in Nuclear Energy, 49*(3), 253–261.

Khan, R., Karimzadeh, S., & Boeck, H. (2009, March). TRIGA fuel burn-up calculations supported by gamma scanning. Paper presented at the Research Reactor Fuel Management (RRFM) Conference, Vienna, Austria.

Khattab, K. (2005). Calculations of fuel burn-up and radionuclide inventory in the Syrian Miniature Neutron Source reactor using the WIMSD4 code. *Annals of Nuclear Energy, 32*(10), 1122–1130.

Matsumoto, T., & Hayakawa, N. (2000). Benchmark analysis of TRIGA Mark II reactivity experiment using a continuous energy Monte Carlo code MCNP. *Journal of Nuclear Science and Technology, 37*(12), 1082–1087.

Melkegna, T. H., Chaubey, A. K., Jonah, S. A., Ahmed, Y. A., & Abubakar, N. (2020). Essential and trace elements status in the indigenous Ethiopian tuber crops. *Radiochimica Acta, 108*(1), 51–56.

Melkegna, T. H., Chaubey, A. K., Beyene, G. A., Bitewlign, T. A., Jonah, S. A., Ahmed, Y. A., & Abubakar, N. (2017). Multi-elemental analysis of indigenous food spices in southern Ethiopia using INAA technique. *Journal of Radioanalytical and Nuclear Chemistry, 314*(3), 1–5.

Moens, L., De Corte, F., Simonits, A., De Wispelaere, A., & Hoste, J. (1979). The effective resonance energy Er as a parameter for the correction of resonance integrals, 1/E(1+α) epithermal neutron spectra: Tabulation of Er for 96 isotopes. *Journal of Radioanalytical Chemistry, 52*(2), 379–387.

Murranka, R. G. (1985). Conversion of research reactors to low enrichment uranium fuel. *IAEA Bulletin, 25*(1), 18–21.

Musa, Y., Ahmed, Y. A., Yamusa, Y. A., & Ewa, I. O. B. (2012). Determination of radial and axial neutron flux distribution in irradiation channel of NIRR-1 using foil activation technique. *Annals of Nuclear Energy, 50*, 50–55.

Qasid, A. S. (2008). Effect of reflector material on neutron calculation of MEU research reactor. *Journal of Al-Nahrain University, 11*(2), 99–104.

Rahgoshay, M., & Noori-Kalkhoran, O. (2013). Calculation of control rod worth and temperature reactivity coefficient of fuel and coolant with burn-up changes for VVR-S 2 MWth nuclear reactor. *Nuclear Engineering and Design, 256*, 322–331.

Ravnik, M. (1990). Nuclear safety parameters of mixed TRIGA cores. In *Proceedings of the Workshop on Reactor Physics Calculations for Applications in Nuclear Technology* (pp. 398–421). International Centre for Theoretical Physics.

Ravnik, M., Strebl, M., Böck, H., & Mele, I. (1992). Burn-up determination of TRIGA fuel elements by calculation and reactivity experiments. *Kerntechnik, 57*(5), 291–296.

Shi, S. (1990). Low power research reactor thermal hydraulics. IAEA Workshop on Low Power Research Reactor. China Institute of Atomic Energy, Beijing.

Souza, R. M. G. P., & Moreira, J. M. L. (2006). Power peak factor for protection systems – Experimental data for developing a correlation. *Annals of Nuclear Energy, 33*(7), 609–621.

Sobes, V., Forget, B., & Kadak, A. (2011). Individual pebble temperature peaking factor due to local pebble arrangement in a

pebble bed reactor core. *Nuclear Engineering and Design, 241*(1), 124–133.

Tayefi, S., & Pazirandeh, A. (2013). Evaluation of applying axial variation of enrichment distribution method and radial variation of enrichment distribution in VVER/1000 reactor using a Hopfield neural network to optimize fuel management. *Progress in Nuclear Energy, 64*, 47–53.

Yahaya, B., Ahmed, Y. A., Balogun, G. I., & Agbo, S. A. (2017). Estimating NIRR-1 burn-up and core life time expectancy using the codes WIMS and CITATION. *Results in Physics, 7*, 596–603.

Declaration

Funding sources

No funding

Competing Financial Interests Statement:

There are no competing financial interests in this research work.

Ethical considerations

Not applicable

Data availability

The microcontroller source code and any other information can be obtained from the corresponding author via email.

Authors' Contribution

AMS conducted experiments, performed data analysis, developed the computer program, and drafted the manuscript. JIA assisted in measurements, data validation, and literature review. YAA conceived the study, supervised the research, guided methodology, and critically revised the manuscript. NR supported reactor operations, instrumentation, and thermal–hydraulic analysis. JAY contributed to computational implementation, results interpretation, and manuscript editing.